Impact of sensor housing geometries onto transient stagnation pressure measurements in supersonic flows

M. Giglmaier[1]*, A. Obrecht[1], Z. Wang[1], T. Hopfes[1], N. A. Adams[1]

[1] Institute of Aerodynamics and Fluid Mechanics, Technical University of Munich

Boltzmannstr. 15, D-85748 Garching bei München, Germany

*marcus.giglmaier@aer.mw.tum.de

Abstract

In the present study, we investigate the characteristic behavior of two different housing geometries for pressure sensors in supersonic flows. Pressure sensors shielded with conical and flat shrouds are positioned radially along the cross section in a shock tube and intended to measure the stagnation pressure of the post-shock flow. The rise time, the oscillating behavior and the absolute value of the signals are compared. Results indicate that pressure measured for both housing geometries experiences oscillations to some extent and settles down at the expected value in the end. However, the signal for the sensor with the conical shroud oscillates at a much larger amplitude through a significantly longer settling time. Numerical simulations are used to support the analysis of the recorded results and to explain internal flow phenomena. Furthermore, we will describe the ongoing experiments visualizing the flow field around the sensor housing using high-speed schlieren photography. Also introduced are the projected experiments concerning the specific sensitivity of the housing geometries to manufacturing tolerances, mounting errors like misalignment to the flow direction and measures to reduce the signal rise time by filling cavities with grease.

1 Introduction

Accurate measurement of the total pressure in supersonic flows is a delicate, but well-known problem since the deceleration of supersonic flows to stagnation conditions typically involves the formation of shocks and hence, total pressure losses. To take them into account, a common way is to use a sensor directed towards the incoming flow and to assume that the center of the involved detached bow shock fulfills the normal shock relations. Then, the ratio of static pressures p_2/p_1 across the shock

$$\frac{p_2}{p_1} = 1 + \frac{2\kappa}{\kappa + 1}(M_1^2 - 1)$$

and the Mach number M_2 behind the shock are solely dependent on the upstream Mach number M_1 and the heat capacity ratio κ of the gas (Anderson, 2002):

$$M_2^2 = \frac{1 + \frac{\kappa - 1}{2} M_1^2}{\kappa M_1^2 - \frac{\kappa - 1}{2}}$$

By assuming an isentropic deceleration downstream of the shock, the stagnation pressure p_{01} of the incoming flow can be expressed as a function of the stagnation pressure p_{02} downstream of the shock and the Mach number M_1 of the undisturbed incoming flow:

$$p_{01} = p_{02} \left(1 + \frac{2\kappa}{\kappa+1}(M_1^2 - 1)\right)^{\frac{1}{\kappa-1}} \left(1 - \frac{2}{\kappa+1}\left(1 - \frac{1}{M_1^2}\right)\right)^{\frac{\kappa}{\kappa-1}}$$

However, the flow directly at the abutting surface accelerates from the stagnation point in the center to Mach number $M = 1$ at the corner of the blunt body as shown in fig. 1a. Consequently, the area-averaged pressure differs slightly from the stagnation pressure and hence, it gives an improper value to calculate the stagnation pressure of the incoming flow.
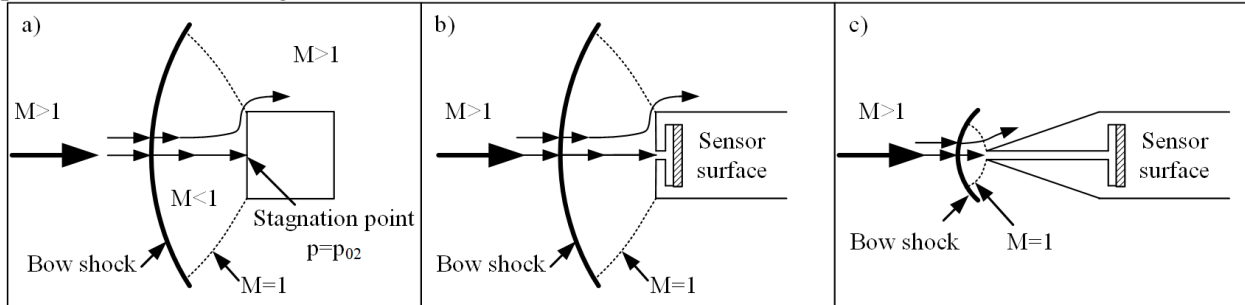

Figure 1: Transonic flow conditions around a blunt body (left), sensor with a flat shroud (middle) and conical shroud (right).

For the measurement itself, piezoelectric or piezoresistive pressure sensors are widely adopted in high-speed flows due to their short response time and high resonant frequency paired with the ability to measure even small pressure fluctuations. When applied in impulse facilities such as shock tubes and expansion tubes, these expensive transducers are generally mounted with a shroud in order to protect them from being destroyed by the fast-travelling fragments of metal diaphragms (Sutcliffe & Morgan 2001). As seen in fig. 1b and fig. 1c, such shielding designs normally create an internal cavity connecting the sensor surface to the ambient flow. A consequence of such cavities is that an incoming unsteady shock wave propagates into the cavity, reflects at the sensor surface, travels back and interact with the ambience of the cavity. This process repeats until the wave dynamics are dampened due to viscous effects.

A high pressure gradient across the incoming shock in combination with an inappropriate geometry results in even slower signal rise time: In the case of sonic flow conditions within the borehole of the sensor cover, the mass flow into the cavity is limited. Thus, the pressure rises slowly if the volume of the cavity is comparably large. Another drawback is, that the sensor is acoustically disconnected from the ambience until a certain pressure in the cavity is reached and the flow in the borehole is decelerated to subsonic flow speed. Also, as demonstrated e.g. by McGilvray et al. (2009), such cavities behave like a Helmholtz resonator and thus introduce noticeable fluctuations to the pressure signals. Considering, that the time window for experiments in impulse facilities tends to be extremely short, methods to reduce the rise time and dampen the pressure fluctuations are desired.

2 Experimental setup

The current experimental research is carried out in a shock tube. As depicted in fig. 2, the shock tube is composed of a driver section (3 m), a driven section (19.5 m) and a test section (0.4 m) attached to the end. The inner cross section has a diameter of 290 mm and changes to a square with the side length 190 mm by a cookie-cutter in front of the test section. A diaphragm, which initially separates the driver section and the driven section, breaks as soon as a critical pressure difference is reached. Subsequently, a shock wave develops and propagates rapidly towards the downstream test section.

As for the measurement system, pressure gauges and K-type thermocouples measure the initial experimental conditions, and a NI cDAQ device collects the signals. Flush-mounted fast-response pressure sensors along the driven section as well as the test section monitor the shock wave inside the tube. A LTT device records the pressure data at a sampling rate of 4 MHz to determine the shock speed accurately. To visualize the flow around the sensors, a Z-type schlieren system is applied. A 150 W Xenon lamp serves

as the light source and a Shimadzu HyperVision HPV-X ultra-high-speed camera records 128 continuous images with a resolution of 250×400 pixels at a framing rate of up to 5 MHz.
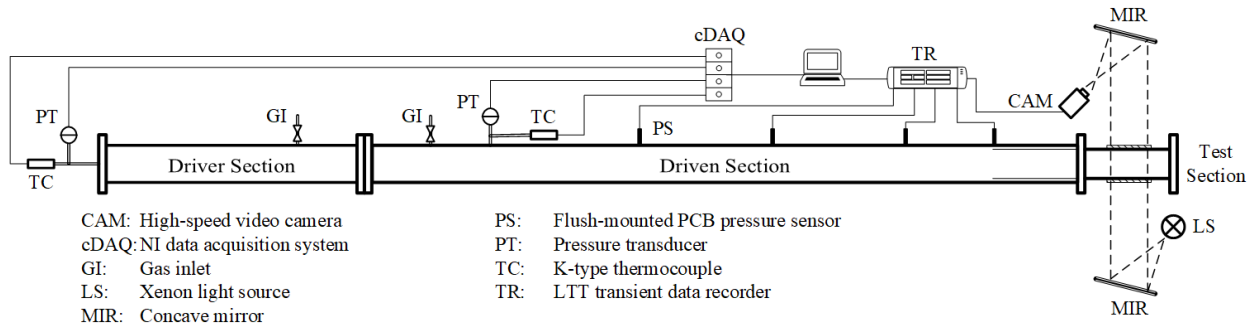

Figure 2: Experimental arrangement of the shock tube (Wang et al., 2018).

For the sensors, two types of shrouds are employed and their impact onto the total pressure measurement of the post-shock conditions is analyzed. In preliminary experiments, the pressure distribution behind the planar shock front is measured via a rack of Pitot probes as depicted in fig. 3. Each Pitot probe is equipped with a PCB Piezotronics ICP® fast-response pressure transducer (Model 113B21) with a resonant frequency above 500 kHz and a rise time below 1 µs. The sensors are mounted in either conical shrouds or flat-head shrouds, of which the former is in a conical shape with an angle of 15° relative to the centerline and has a longer and broader cavity (diameter of 2 mm and length of 17 mm) compared to the latter (diameter of 1 mm and length of 1 mm). Cables are hidden inside the closed joint triangle housings and connected to the LTT transient data acquisition device.

A similar approach as depicted in fig. 3 will be used for the experiments with optical access. Two sensors are directed towards the incoming flow and two sensors are inclined by 2°. Thus, both types of sensor covers and their sensitivity to mounting errors can be analyzed under equal experimental conditions.
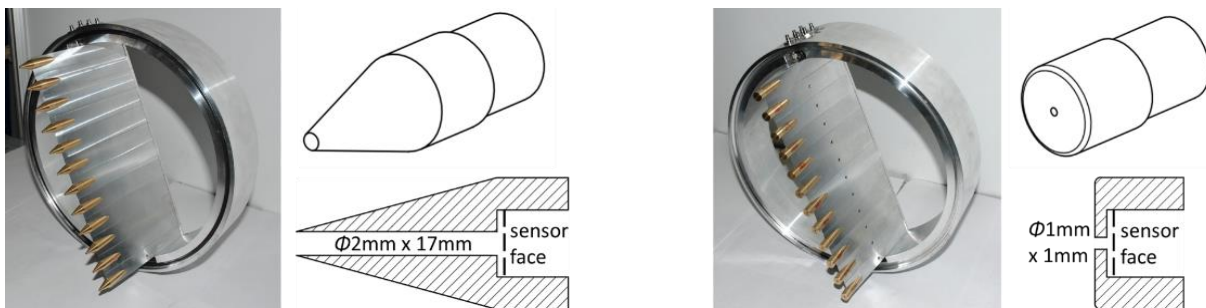

Figure 3:Experimental Pitot rack for the measurement of the total pressure profile in the shock tube and simplified sensor shroud sketches: sharp-head shrouds left and flat-head shrouds on the right.

3   Preliminary results

For the following results, the Pitot rack was equipped with six flat and six conical sensor covers in order to analyze their behavior under equal experimental conditions. The operating pressure in the driver section ranges between $p_4=7,2\cdot10^5$ Pa and $p_4=8,1\cdot10^5$ Pa and the applied pressure in the driven section ranges from $p_1=1,1\cdot10^2$ Pa to $p_1=9,6\cdot10^4$ Pa. The measured pressure signals for the different sensor covers are given in fig. 4 and fig. 5 together with the corresponding operating pressure ratio and the measured shock Mach number M_S. In all cases, the measured pressure is normalized by the according theoretical value.

As can be seen in fig. 4 on the left side, the signals from the sensors with a conical shroud are rising slowly at the beginning and reach a maximum after $\Delta t=80\text{-}140$ µs followed by large-amplitude oscillations. The signals settle down gradually to a stable value as the oscillations diminish and the overall settling time varies between $\Delta t=350\text{-}1000$ µs. The amplitude of the oscillations decreases for increasing pressure ratios due to

the decreasing Reynolds number. In contrast, the dominant frequency of the oscillations changes only gradually between f=3700 Hz and f=4800 Hz as can be seen in the corresponding frequency spectra in fig. 4 on the right. Besides the broad peak at a comparatively low frequency, three minor peaks occur at f=13-16 kHz, f=22-24 kHz and f=136 kHz.
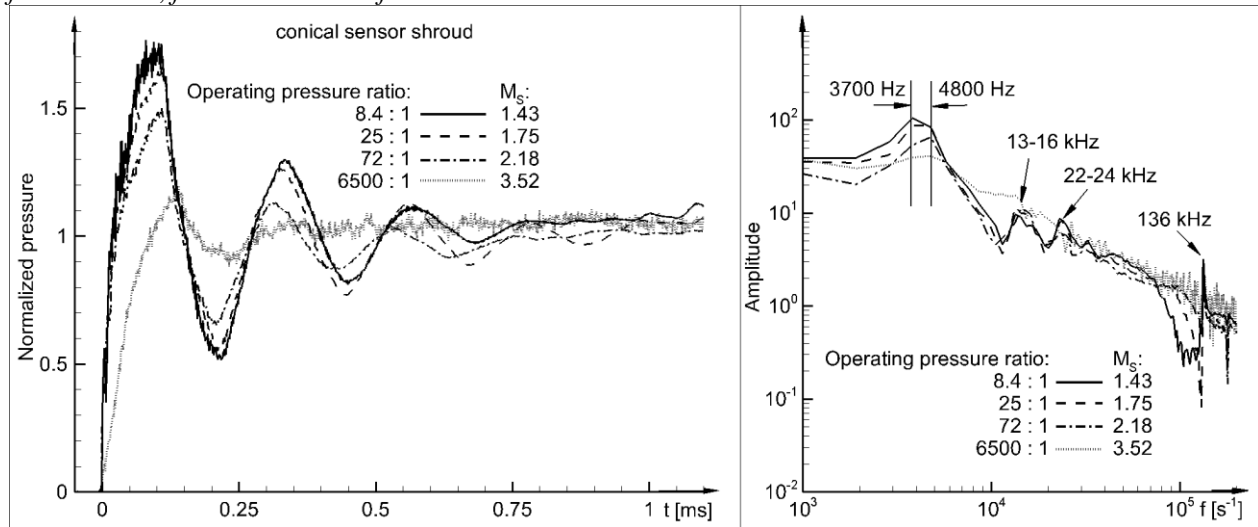

Figure 4: Measured pressure signals (left) and according frequency spectra (right) of the sensors with conical shrouds.

In comparison, fig. 5 shows the corresponding pressure plots for the experiments with the flat sensor covers. At first, the signals exhibit overshoots of similar intensity but in contrast, they decay rapidly to the expected value. The overall rise time, until a stable pressure is reached, varies only between Δt=50-150 μs. The frequency spectra are much flatter and only the experiments with higher Reynolds number exhibit pronounced peaks at f=17.4 kHz and f=19.3 kHz. The higher frequency for these peaks was expected due to the shorter borehole length. The small peak at f≈133 kHz that can also be detected for the experiments with a conical shroud presumably corresponds to the cavity size behind the borehole.
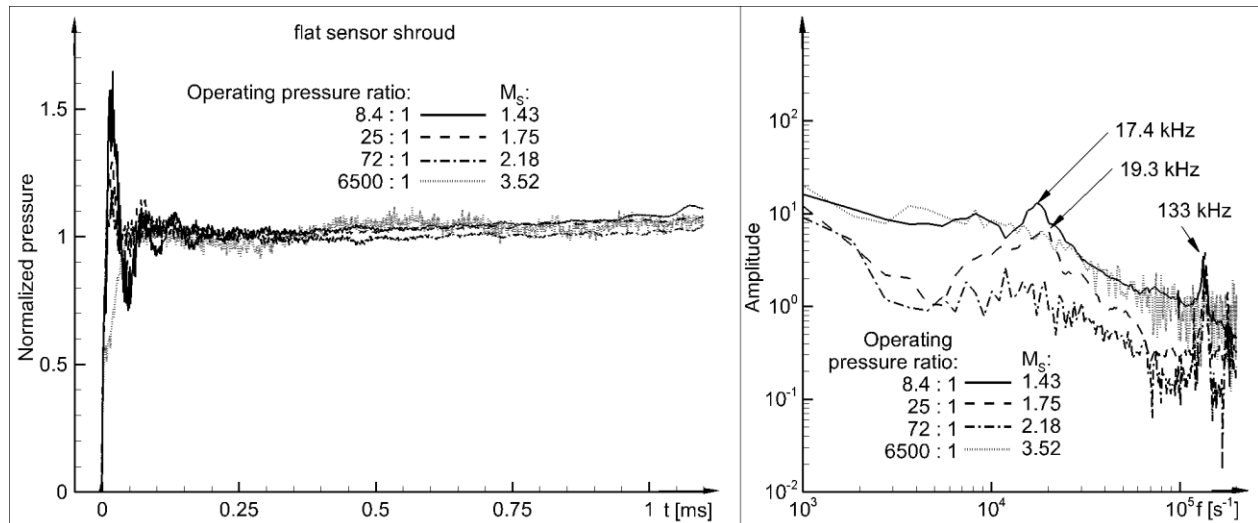

Figure 5: Measured pressure signals (left) and according frequency spectra (right) of the sensors with flat shrouds.

A CFD-simulation executed prior to the design of the sensor covers already predicted the experimentally obtained behavior, as can be seen in fig. 6. The boundary conditions of this simulation correspond to a pressure ratio of 1000 to 1. The absolute pressures (10^6 Pa in the driver section, 10^3 Pa in the driven section) and the geometry of the sensor covers slightly differ and hence, a small difference in the calculated

frequency spectra is to be expected. Nevertheless, the overall behavior is similar and the simulations are suitable to further analyze and explain the flow physics inside the cavities. Therefore, further detailed simulations are planned.
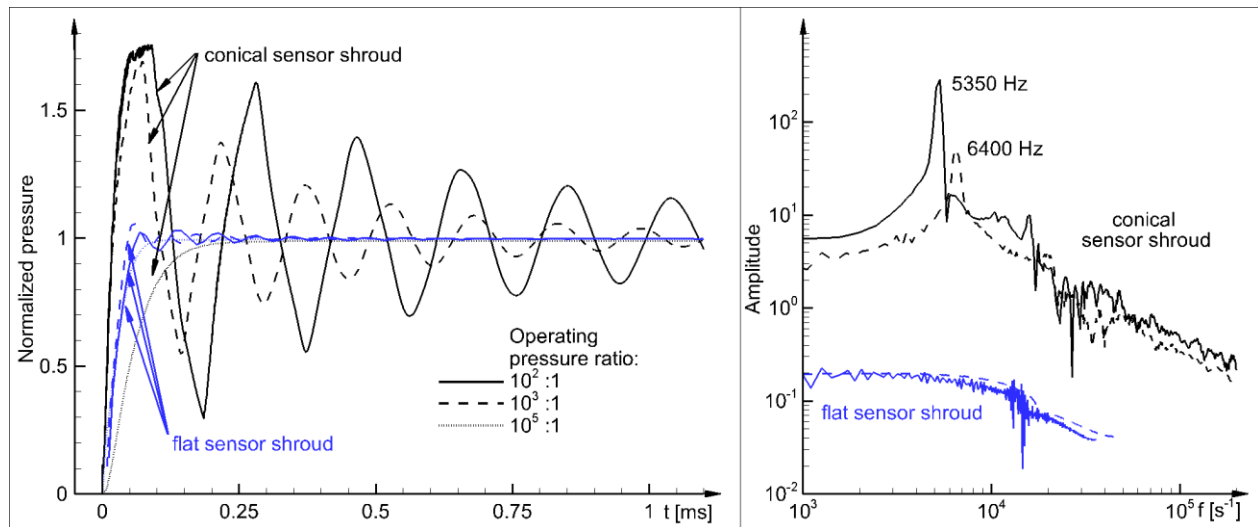

Figure 6: Simulated pressure distributions for different sensor shrouds (left) and according frequency analyses (right).

4 Outlook

Distinct differences are observed between the performances of two types of shrouds. More experiments under a wider range of pressure conditions will be conducted to analyze the rise time, Eigen frequency and absolute pressure value coming along with the individual cavity length, cavity height and shroud shape. Furthermore, multiple Pitot tubes with different angles of attack will be analyzed simultaneously in a test chamber with optical access in order to evaluate their sensitivity to mounting errors. High-speed schlieren videos with 5 Mfps (Camera: Shimadzu HPV-X) will help to examine the transient evolution of the flow field around single Pitot probes. Finally, the impact of filling cavities with grease will be investigated with respect to response time and measured absolute pressure values.

References

Anderson, J. D. (2002): Modern Compressible Flow. McGraw-Hill Science Engineering, New York, ISBN 0-07 112161-7.

McGilvray, M., Jacobs, P. A., Morgan, R. G., Gollan, R. J., Jacobs, C. M. (2009): Helmholtz resonance of Pitot pressure measurements in impulsive hypersonic test facilities. *AIAA Journal*, *47*(10), 2430-2439.

Sutcliffe, M. A., & Morgan, R. G. (2001): The measurement of Pitot pressure in high enthalpy expansion tubes. Measurement Science and Technology, 12(3), 327.

Wang, Z., Hopfes, T., Giglmaier, M., Adams, N. A. (2018): Experimental investigation on destructive potential of shock-induced bubble collapse. International Symposium on Cavitation (CAV2018).